Nuclear Instruments and Methods in Physics Research B 273 (2012) 226–230

Contents lists available at SciVerse ScienceDirect

Nuclear Instruments and Methods in Physics Research B

journal homepage: www.elsevier.com/locate/nimb

High brilliance multicusp ion source for hydrogen microscopy at SNAKE

M. Moser [a,*], P. Reichart [a], W. Carli [b], C. Greubel [a], K. Peeper [a], P. Hartung [b], G. Dollinger [a]

[a] Universität der Bundeswehr München, Institut für Angewandte Physik und Messtechnik, LRT2, Department für Luft- und Raumfahrttechnik, 85577 Neubiberg, Germany
[b] Maier-Leibniz-Laboraturium der LMU und TU München, 85478 Garching, Germany

ARTICLE INFO

Article history:
Available online 27 July 2011

ABSTRACT

In order to improve the lateral resolution of the 3D hydrogen microscopy by proton–proton scattering at the Munich microprobe SNAKE, we have installed a new multicusp ion source for negative hydrogen ions manufactured by HVEE at the Munich 14 MV tandem accelerator that boosts the proton beam brilliance with the potential to reduce the beam diameter at the focal plane of SNAKE. We measured a beam brilliance $B = 27\ \mathrm{A\,m^{-2}\,rad^{-2}\,eV^{-1}}$ directly behind the ion source that is at the space charge limit for conventional ion sources. After preacceleration to in total 180 keV beam energy we measure a slightly reduced beam brilliance of $B = 10\ \mu\mathrm{A\,mm^{-2}\,mrad^{-2}\,MeV^{-1}}$. For injection into the tandem accelerator, the extracted H^--current of the multicusp source of 1 mA is reduced to about 10 μA because of radiation safety regulations and heating problems at the object slits of SNAKE. Due to beam oscillations and influences of the terminal stripper of the tandem we measured a reduced beam brilliance of $0.8\ \mu\mathrm{A\,mm^{-2}\,mrad^{-2}\,MeV^{-1}}$ in front of SNAKE at 25 MeV but still being nearly 10 times larger than measured with any other ion source.

1. Introduction

Proton–proton scattering has proven as an ideal method for detection of hydrogen. When utilizing protons with energies from 10 MeV to 25 MeV at the Munich microprobe SNAKE it is even possible to sensitively and quantitatively analyze hydrogen in microstructured materials [1–3]. A detection limit of less than 1 ppm and a lateral resolution of about 1 μm makes it a unique method to perform quantitative hydrogen microscopy. By analyzing the energy of the protons we get in addition a depth resolution of a few micrometers and thus can perform microscopy in three dimensions (3D hydrogen microscopy). In many materials scientists are interested in the 3D distribution of the hydrogen content. E.g. in geologic samples one searches for gradients of the hydrogenin micrograined material from the earth mantle [4] or metallurgists search for hydrogen on grain boundaries in metals [5,6]. We were the first to detect hydrogen at grain boundaries of polycrystalline diamond [7].

In many applications the search for small contents of hydrogen in microstructures is limited by the lateral resolution since small amounts of hydrogen become below the detection limit because the profiles are smeared out. In addition, lateral structures with structure sizes in the few micrometer range cannot be well imaged due to the limited lateral resolution. Thus the aim of our actual work is to reduce beam diameters in order to enhance lateral resolution.

The optimum lateral resolution we obtained for hydrogen microscopy at the Munich ion microprobe SNAKE was $0.6 \times 2\ \mu\mathrm{m}^2$ using the existing ECR source for H^--ions [8] and optimum beam transport through the accelerator and SNAKE [7]. This value is mainly given by the beam diameter on target while other parasitic effects have been shown to contribute less than 0.5 μm [9]. In order to obtain smaller beam diameters we have to increase the brilliance B of the beam that is given by

$$B = I/(\Delta x\,\Delta\varphi_x\,\Delta y\,\Delta\varphi_y E). \tag{1}$$

Here the beam brilliance B is defined non-relativistically as the ratio of the ion current I and the transversal phase space volume divided by double the mass m of the ions as it is usually done in the field of ion beam analysis:

$$\Delta x\,\Delta p_x\,\Delta y\,\Delta p_y/(2m) = (\Delta x\,\Delta\varphi_x\,\Delta y\,\Delta\varphi_y)E. \tag{2}$$

The beam brilliance B characterizes the beam and is a constant value under ideal beam transport and acceleration conditions. The main parameters are the minimum diameters of the beam in its focus Δx and Δy and the transversal momenta Δp_x and Δp_y at this beam focus. These transversal momenta can be determined through the divergences $\Delta\varphi_x$ and $\Delta\varphi_y$ of the beam: $\Delta p_x\,\Delta p_y/(2m) = \Delta\varphi_x\,\Delta\varphi_y E$.

In order to improve beam resolution one needs to reduce the object slits widths Δx and Δy of SNAKE and to reduce beam aperture and thus $\Delta\varphi_x$ and $\Delta\varphi_y$ in front of SNAKE in order to reduce the influence of spherical lens aberrations, thus reducing the transversal phase space volume of the beam. However, this reduction also reduces beam current, but the required current of about 100 pA

* Corresponding author.
E-mail address: marcus.moser@unibw.de (M. Moser).

0168-583X/$ - see front matter © 2011 Elsevier B.V. All rights reserved.
doi:10.1016/j.nimb.2011.07.081

has to be conserved, because count rate for hydrogen detection has to be kept in particular for microprobe imaging. To achieve the same beam current at reduced phase space volume of the beam, the only way is to increase the brilliance of the beam. Since the phase space volume of an ion beam cannot be improved by conventional beam transport systems due to Liouvilles law the easiest way to enhance beam brilliance is to enhance the brilliance of the ion source. External beam cooling, e.g. through interaction of the proton beam with a high brilliant electron beam, is considered to be too expensive.

With the ECR source that already existed at the Munich tandem accelerator we measured an optimum brilliance of $B = 0.1\ \mathrm{A\,m^{-2}\,rad^{-2}\,eV^{-1}}$ at SNAKE [8]. Raytracing simulations of the optimum lens design at SNAKE demonstrate, that a brilliance of $B = 1\ \mathrm{A\,m^{-2}\,rad^{-2}\,eV^{-1}}$ is required for a resolution of 100 nm in both directions getting a beam current of 100 pA at the experiment under ideal conditions [10]. The raytracing calculations indicate [10] that the reduction of beam divergence at SNAKE improves more than quadratically the beam resolution. Thus we installed a new high brilliance multicusp H^--source from High Voltage Engineering Europe (HVEE) [11] with a specified brilliance of $15\ldots20\ \mathrm{A\,m^{-2}\,rad^{-2}\,eV^{-1}}$, that in fact was beaten at the acceptance test at manufacturers site with $B = 27\ \mathrm{A\,m^{-2}\,rad^{-2}\,eV^{-1}}$. The improved beam brilliance will lead to smaller beam sizes although lens imperfections and AC-stray fields will still limit beam resolution.

2. System description

The new high brilliance multicusp ion source is included at the low energy side of the Munich 14 MV tandem accelerator which is illustrated in Fig. 1. The source is installed on a platform that delivers all required infrastructure for electrical power and water cooling at a negative potential for the preacceleration of e.g. 150 kV that adds to the source extraction potential of $U_{Ex} = 30$ kV. Thus, after preacceleration, the ions have a total energy of 180 keV.

2.1. Design of the multicusp ion source for the 14 MV tandem accelerator

The physical principle and construction of the source is discussed in detail in [12]. Here, we just want to summarize the main issues of the multicusp ion source in producing negative hydrogen ion beams with highest brilliance. The concept of the installed source is shown in Fig. 2 including its electric configuration. The electric parameters to run the multicusp ion source under stable conditions are summarized in Table 1.

Left to the extraction electrode Fig. 2 shows a schematic drawing of the multicusp source as manufactured by HVEE. A cathode with its tungsten filament produces a high current of 50 A of electrons at a potential of −100 V relative to the anode formed by a metallic cylinder to run an hydrogen plasma. The multipole field forces constrain the electrons to cycle within the cylinder filled

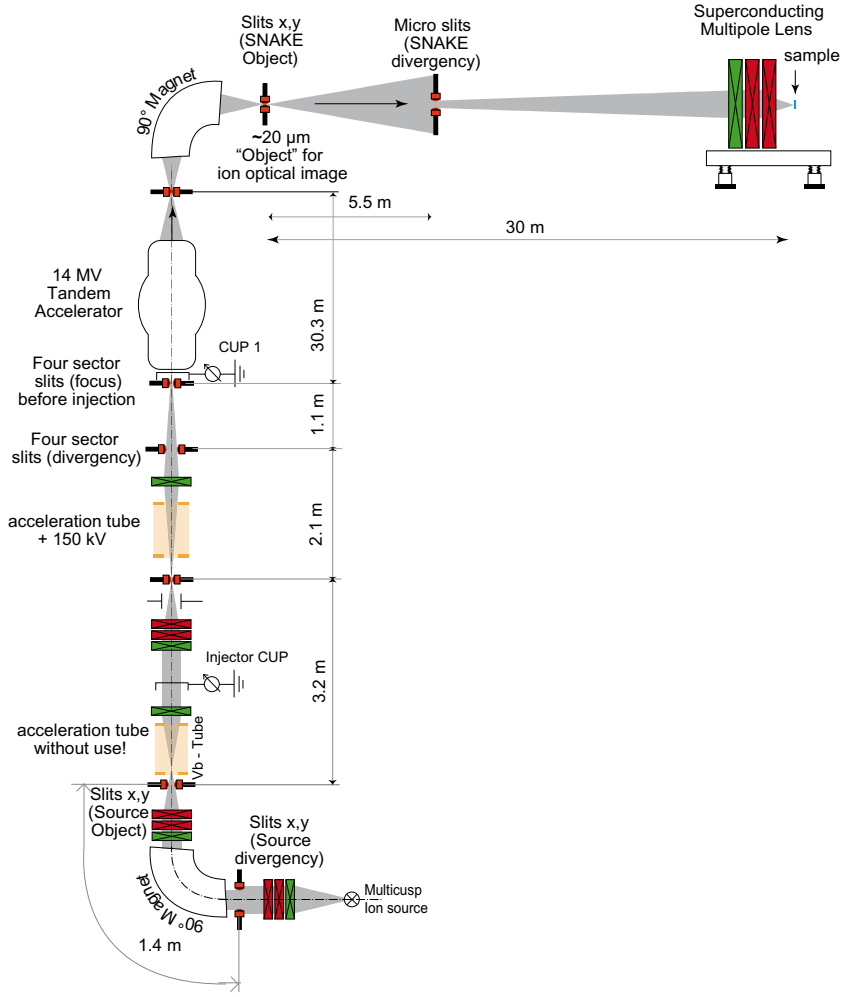

Fig. 1. Illustration of the whole beam line (without scaling of the lengths) with the important values of the lengths from the ion source to the experiment.

with hydrogen gas at $p = 50$ Pa. The electrons drift axially losing their kinetic energy until they reach the optimum energy of about 1 eV in front of the extraction bore in order to create a high density of H^--ions [12]. Attachment yield of electrons to neutral hydrogen atoms is much larger at these low energies than destruction of already formed H^--ions by electron impact [12]. Thus a high density of H^--ions are formed close to the extraction bore that leads to a space charge limited brilliance of $B = 27$ A m^{-2} rad^{-2} eV^{-1}.

The space charge limit by well known Child–Langmuir law results from the shielding of the acceleration field by the emitted ion beam giving a natural limit of the resulting brilliance of a beam. The maximum brilliance of a charged particle beam extracted through an aperture of radius r and a distance of the acceleration electrodes d is given by this limit [13]:

$$I_{Ex} = \frac{4\pi}{9}\epsilon_0\sqrt{\frac{2q}{m}}S^2U_{Ex}^{\frac{3}{2}} \quad (3)$$

with $S = r/d$ being the aspect ratio, ϵ_0 the dielectric constant and q/m the specific charge of the extracted ions. Assuming a simplified model of the extraction geometry of the multicusp ion source we have $r = 2.5$ mm and $d = 68$ mm and thus $S = r/d = 0.036$. The maximum beam current I_{Ex} that can be obtained with this geometry is plotted in Fig. 3 in dependence of the applied acceleration voltage.

We indicate also the point of measured ion current of $I_{Ex} = 965$ - μA at an acceleration voltage of 30 keV that is very close to the estimation of the space charge limited ion current. This means that there is not an easy way to improve the current at the given geometry and thus to improve the brilliance of the beam in general beside increasing the extraction voltage U_{Ex}. But technical limits are set to $U_{Ex} \leqslant 30$ kV.

There are several limits in using the H^--beam that is extracted from the multicusp ion source at the Munich tandem accelerator. One major difficulty arises because one cannot inject the high currents of $I = 1$ mA into the tandem accelerator due to the existing power supplies, limiting charging currents of the tandem accelerator, radiation restrictions and heating of microslits in front of SNAKE. For instance, a 1 mA proton beam virtually fed through the tandem accelerator to produce proton energies of 20 MeV would make a heat load of 20 kW on the first microslits of the SNAKE microprobe and a neutron dose rate at the front edge of the accelerator both about 100 times larger than can be accepted with the existing installations. The actual microslit system at SNAKE is even only able to withstand beam currents smaller than 1 μA. The 1 mA is already a lower current of the multicusp than the originally specified 1.5 mA by reducing the extraction aperture of the first electrode from $2r = 7$ mm ($S = 0.052$) to $2r = 5$ mm ($S = 0.036$) in accordance with the Langmuir law equation (3). The measured reduction of total current to 750 μA when extracting negative deuterium from the actual source geometry is also in accordance with Eq. (3). In order to further reduce the beam current for injection into the tandem without disturbing the beam brilliance we introduce two pairs of slits directly behind the source in order to reduce the beam divergences $\Delta\varphi_x$ and $\Delta\varphi_y$. In order to do so we installed a transfer box behind the source that is also shown in Fig. 2 on the right hand side of the extraction electrode.

Table 1
Summary of the electrical concept including the necessary power of the power supplies with optimized system parameters to run a stable proton beam from the multicusp.

Element	Voltage U (V)	Current I (A)	Power P (W)
Filament	7	150	1050
Anode	100	30	3000
Electrode 1	2.5	17	42.5
Elektrode 2	3350	20×10^{-3}	67
Extraction	−25,580	1.3×10^{-3}	33

The transfer box contains also a pair of magnetic steerers, an electrical quadruple and an electrostatic Einzel lens to adjust the beam to the optical axes and to the beam optics at the low energy side of the tandem accelerator.

Behind the extraction box there follows a doubly focusing 90° magnet to transfer the beam onto the beam axis of the low energy

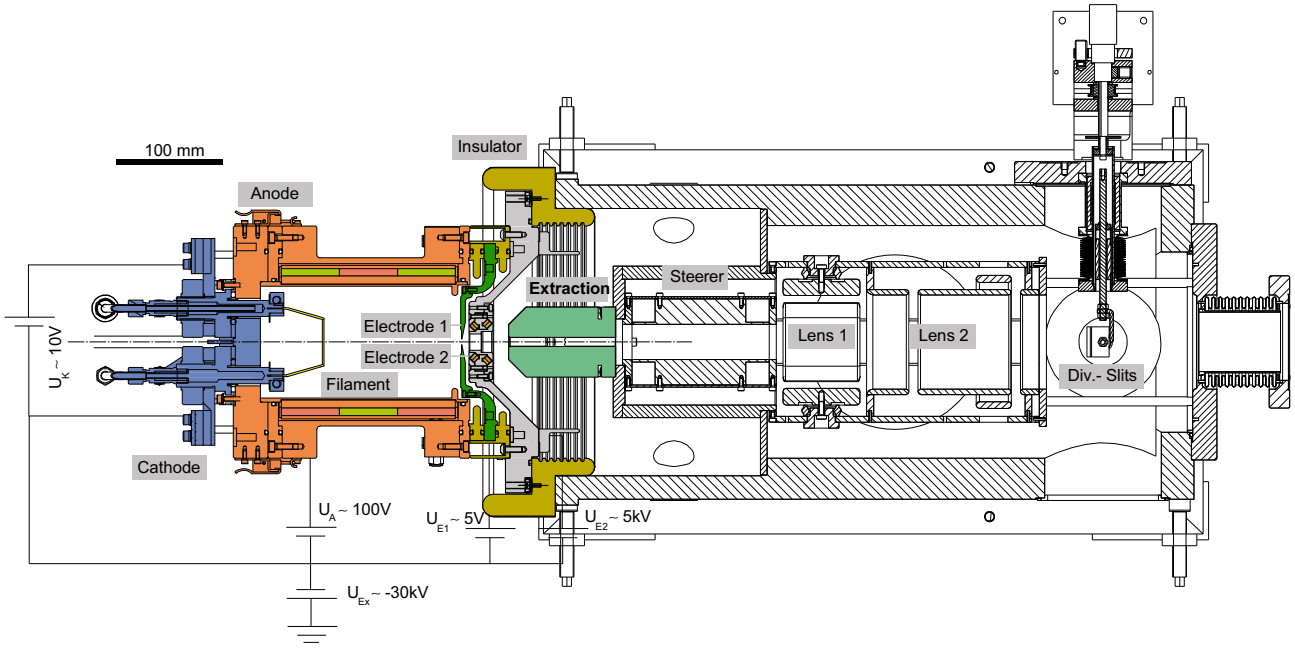

Fig. 2. Illustration of the high brilliance multicusp H^--ion source with its extraction system as installed at the Munich tandem accelerator. Also shown is the electrical concept of the source with its potentials. Behind the extraction electrode (green) there is installed a beam transfer box containing a pair of steerers to correct the direction of the beam followed by an electrostatic and a quadrupole lens to tune the focusing system and its astigmatism. At the end of the transfer box there is are two pairs of slits for defining the divergences of the beam to reduce the total injected current keeping the beam brilliance. After the extraction box there is the injection magnet to lead the beam onto the ion optical axes of the tandem accelerator. (For interpretation of the references to color in this figure legend, the reader is referred to the web version of this article.)

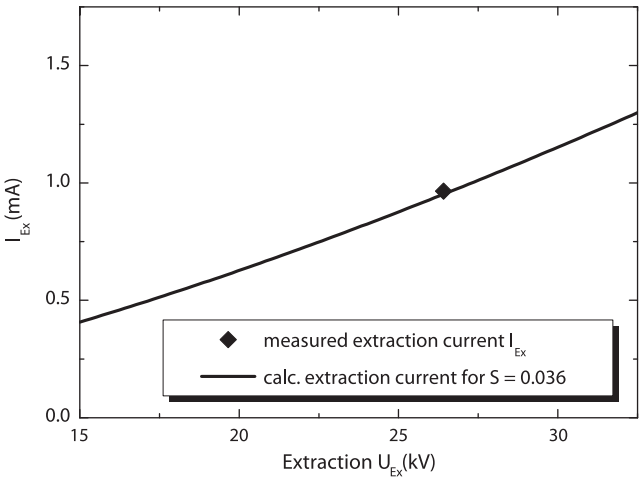

Fig. 3. Calculated space charge limited extraction current I_{Ex} depending on the extraction voltage U_{Ex} after Eq. (3) for different aspect ratios of $S = 0.036$. There is also plotted the measured extraction current.

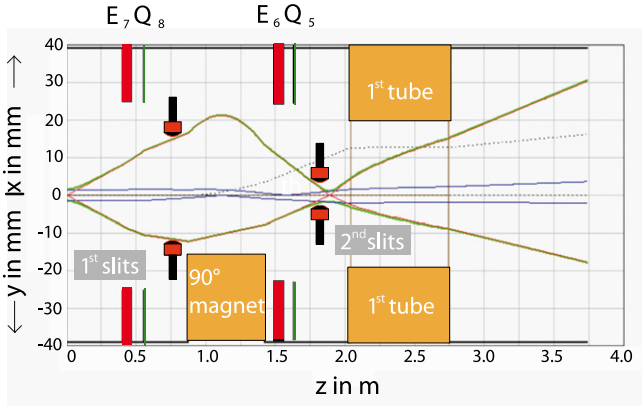

Fig. 4. Calculation of beam transport after beam extraction before injection into the 14 MV tandem accelerators. The positions of the optical lenses for correction of the beam direction and the both slits systems are displayed, the first to reduce divergences and the second at the beam focus for defining an object for further beam transport.

stage of the tandem accelerator. Fig. 4 shows a raytracing calculation of the beam after extraction of the source for injection to the low energy stage of the tandem accelerator. It shows the beam transport through the optical lenses in front and behind the 90° injection magnet and two slits systems. The first pair of slits are the already mentioned divergence slits situated in the transfer box in front of the 90° magnet and one pair of slits is placed near to the focus behind the 90° double focusing magnet cutting the beam size at this focal position (Δx, Δy). Behind this second pair of slits preacceleration follows already with the beam current reduced to less than 20 μA.

For stable operation the controlled process variable is the anode voltage which should always be 100 V to operate the source on this value the filament current has to be adjusted.

3. Brilliance measurements

Fig. 1 shows the whole beam line schematics from the new high brilliance multicusp proton source through the Munich tandem accelerator to the experiment SNAKE. The scaling of the dimensions varies for the different sections of beam transport. We measured the beam brilliance of the proton beam after preacceleration in front of the tandem accelerator and behind the 90° analyzing magnet within the SNAKE transport line. In order to avoid problems of too high currents we performed the brilliance measurements with the beam chopped in front of the Tandem accelerator by a rectangular driven electrostatic chopper that produces 100 ns long beam pulses that were separated by 800 ns. Together with the already reduced beam current of 13 μA in front of the accelerator we worked with the save average beam current of 1.5 μA. All values given in the following are scaled to the full current without chopper action.

3.1. Brilliance before injection

We measured the brilliance of the proton beam before injection into the tandem accelerator with the help of two four-sector slit systems which define the phase space of the beam before injection into the tandem. The slits were reduced as far as that the beam current shows a quadratic reduction with aperture opening. We calculate an emittance of $\varepsilon = 0.7$ mm 1.26 mrad·$\pi = 0.88\pi$ mm mrad at a beam energy of $E_{in} = 173$ keV (extraction voltage of $U_{Ex} = 23$ kV for this case and a preacceleration potential of $U_{preacc} = 150$ kV). With the emittance ε, the measured beam current and energy we get a brilliance of $B = 10$ μA mm^{-2} mrad^{-2} MeV^{-1}.

3.2. Brilliance at SNAKE

In order to measure the emittance and brilliance behind the tandem accelerator and its analyzing magnet we used the microslits system of SNAKE (see Fig. 1). The beam is focused onto the first microsilts that gives the object for the optical demagnification for SNAKE ("object slits") in x- and y directions. The divergence slits were reduced until the beam current shows a quadratic reduction with beam apertures. For the object slits we used a size of 200×200 μm^2 and the divergence slits were reduced to a size of 1000×1000 μm^2 at a distance of $d = 5.5$ m from the object slits. We obtained a maximum current of $I_{Target,DC} = 17$ nA at the target position of SNAKE. This results in a brilliance of $B = 0.8$ μA mm^{-2} mrad^{-2} MeV^{-1} at the high energy side that is about 12 times less than in front of the tandem accelerator.

4. Discussion and conclusion

By installing the multicusp ion source the brilliance of the proton beam at SNAKE was enhanced by about a factor of 10 compared to the proton beams that were available up to now at the Munich tandem accelerator. However, the brilliance at SNAKE is about a factor of 10 less than the brilliance in front of the tandem accelerator and more than a factor 30 less than measured directly behind the ion source. There might be several reasons for this loss in beam brilliance:

- Reduction of beam brilliance due to space charge limits in beam transport.
- Contribution of the stripper to beam divergence due to multiple scattering and energy straggling effects, although this effect was estimated to be a small contribution.
- Beam fluctuations due to the inclined field tubes used in the accelerator in connection with field variations along the acceleration tubes.

The space charge limitations due to beam transport may be only valuable until the preacceleration stage is reached because the effect is reduced similarly with beam energy as it is with the Child–Langmuir space charge limit from the acceleration of the beam

from the source. This effect may account for the reduced beam brilliance in front of the accelerator compared to the values measured directly behind the source. This effect may be even reduced by including an earlier preacceleration directly behind the 90° injection magnet as it will be used in future.

Both of the other effects may be overcome by increasing the phase space value of the beam injected into the tandem accelerator since small angular spreads or beam oscillations have minor influence when a large phase space covers the acceptance of the SNAKE system even if small changes occur. This would mean, however, to transport higher beam currents with the main problems of heat load on the microslits and on the radiation safety regulations. Possible solutions for these problems will be addressed in future.

How far the improved proton beam brilliances will improve the beam resolution has not yet experimentally tested. There is additional effort under way to reduce parasitic effects on beam size like beam oscillations and beam drift at the focal point of SNAKE. The combination of both, reducing the phase space of the beam injected into SNAKE and the enhancement of pointing stability will give the chance to routinely work with submicron lateral resolution for hydrogen microscopy.

References

[1] G. Dollinger et al., Nucl. Instr. and Meth. B 210 (2003) 6–13.
[2] P. Reichart et al., Nucl. Instr. and Meth. B 210 (2003) 135–141.
[3] P. Reichart et al., Nucl. Instr. and Meth. B 219–220 (2004) 980–987.
[4] J. Gose et al., Amer. Miner. 93 (2008) 1613–1619.
[5] A.M. Brass et al., Acta Mater. 44 (1996) 3823–3831.
[6] P.M. Abraham et al., J. Nucl. Mater. 73 (1978) 77–88.
[7] P. Reichart et al., Science 306 (2004) 1537.
[8] R. Hertenberger, Y. Eisermann, A. Metz, P. Schiemenz, G. Graw, AIP Conf. Proc. 570 (2001) 825.
[9] G. Dollinger et al., Nucl. Instr. and Meth. B 231 (2005) 195–201.
[10] G. Hinderer, G. Dollinger, G. Datzmann, H.J. Körner, Nucl. Instr. and Meth. B 130 (1997) 51.
[11] J. Visser et al., Nucl. Instr. and Meth. B 231 (2005) 32.
[12] R.S. Hemsworth, T. Inoue, IEEE Trans. Plasma Sci. 33 (6) (2005) 1799–1813.
[13] C.D. Child, Phys. Rev. 32 (1911) 492. I. Langmuir, ibid. 21 (1921) 419.